Modeling of the Salt and pH Effects on the Permeability of Grafted Porous Membranes

K. Kontturi, S. Mafé,*,† J. A. Manzanares,† B. L. Svarfvar,‡ and P. Viinikka

Department of Physical Chemistry and Electrochemistry, Helsinki University of Technology, FIN-02150 Espoo, Finland

Received April 3, 1996[⊗]

ABSTRACT: A simple theoretical model describing the effects of pH and salt concentration on the permeability and counterion transport number of variable permeability membranes has been presented and validated experimentally for the case of poly(vinylidene fluoride) membranes graft modified with poly(acrylic acid) chains by radiation-induced grafting. The model incorporates explicitly the statistical conformations of a polyacid chain grafted onto the pore surface. The electrostatic interactions between the bound charges in the chains are screened according to the Debye−Hückel theory. The charged capillary model for porous membranes is then used to evaluate the permeability and counterion transport number of the membrane. This theoretical approach is able to describe the experimental trends observed for a range of KCl concentrations and pH values when the grafting ratios are low. In particular, the fact that the membrane permeability changes by several orders of magnitude when the properties of the external solution are varied can be rationalized in terms of very simple physical principles.

I. Introduction

Recent interest in chemomechanical systems[1−5] and chemical valves[2,6−8] has increased significantly the number of studies on the electromechanical properties of polymers and polymer composites. Chemical valves are membranes whose permeability is very sensitive to the electrochemical environment and can thus be controlled by external chemical and physical factors such as the pH, the salt concentration, and the applied electric field.[8−13] This behavior enables the control of water permeability and selectivity with respect to charged species. The membranes have potential biomedical interest because of their biocompatibility, high water permeability, and variable permeability to drug molecules, which could make them suitable for implants and controlled drug release systems. Though most of the studies have dealt with uncharged hydrogels, such as those used in soft contact lenses, polyelectrolyte gels and membranes currently offer very promising applications.[11,14−16]

A convenient way of preparing a variable permeability membrane (VPM) is to modify a porous membrane by grafting monomers possessing functional groups onto the pore surface. The variable permeability can arise, e.g., from the reversible protonation and deprotonation of suitable groups of a polyacid in the membrane, which in turn leads to the reversible contraction and extension of the polyacid chains with the concomitant opening or closing of the pores, as shown in Figure 1. In a previous paper, a complete experimental characterization of poly(vinylidene fluoride) (PVDF) hydrophobic membranes that were graft modified with poly(acrylic acid) (PAA) by radiation-induced grafting was presented.[17] The resulting PVDF/PAA membranes showed a convective permeability which changed significantly with the pH and/or the salt concentration of the bathing aqueous solutions. Gravimetrically determined grafting ratios up to 85% were considered. The morphology of the membranes was characterized with scanning electron microscopy and the membrane electrochemical properties studied were the counterion transport number, the ion-exchange capacity, and the electrical conductivity.[17]

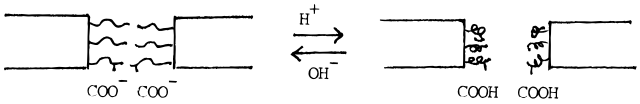

Figure 1. Schematic diagram explaining how expansion of the PAA chains causes the pores to become smaller.

The main purpose of this article is to propose a theoretical model for the permeability of PVDF/PAA membranes with low grafting ratios based on the experimental information now available. The model is very simple and could be applied to other VPM possessing polyacid chains on their pore surface. It is developed for a one-dimensional polyacid chain and incorporates explicitly the entropic and energetic contributions to the chain conformation. The electrostatic interactions between the bound charges in the PAA chains are screened according to the Debye−Hückel theory. The charged capillary model for porous membranes[18] is used to evaluate the permeability and counterion transport number of the PVDF/PAA membrane. The theory can explain most of the experimental trends observed for the membranes with low grafting ratios when the pH and salt concentration of the external solution are changed.

II. Experimental Results

Part of the following experimental results were given in ref 17. Details on the membrane preparation and characterization as well as on the experimental procedures can be found there. Here we will present new data corresponding to the 9% grafting ratio measurements and discuss all the experimental results obtained for the membrane permeability and transport number. Figures 2 and 3 show the dependence of the membrane permeability on the pH and KCl concentration, respectively, for different grafting ratios.[17] The ionic strength was fixed to 100 mM in Figure 2. No HCl was added to the bathing solutions when the measurements in Figure 3 were carried out, so that the pH is ca. 5.8 due to the equilibrium with atmospheric carbon dioxide. Fig-

† Department of Thermodynamics, Faculty of Physics, University of Valencia, E-46100 Burjasot, Spain.
‡ Department of Polymer Technology, Åbo Akademi University, Porthansgatan 3-5, FIN-20500 Åbo, Finland.
⊗ Abstract published in *Advance ACS Abstracts,* July 1, 1996.

S0024-9297(96)00501-3 CCC: $12.00

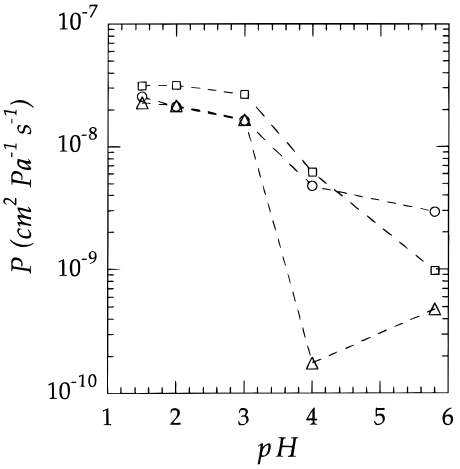

Figure 2. Membrane permeability at constant ionic strength of 100 mM as a function of pH for the grafting ratios 9% (○), 16% (□), and 38% (△).

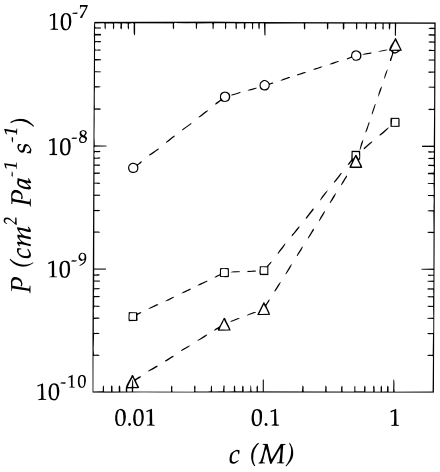

Figure 3. Membrane permeability as a function of KCl concentration with no added HCl (i.e., pH ≈ 5.8) for the grafting ratio 9% (○), 16% (□), and 38% (△).

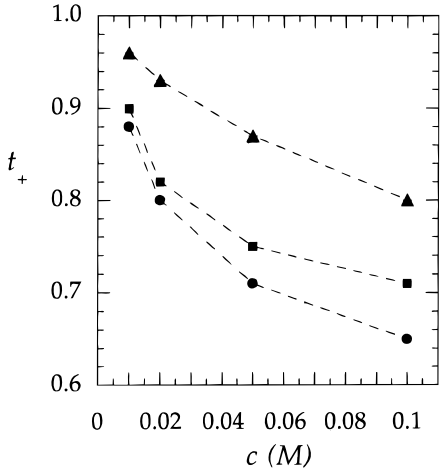

Figure 4. Potassium ion transport number as a function of KCl concentration for different grafting ratios and no added HCl: 8% (●); 12% (■); and 36% (▲).

ures 4 and 5 show the dependence of the counterion (potassium) transport number of the PVDF/PAA membranes on the KCl concentration (for no added HCl, i.e., pH ≈ 5.8) and grafting ratio, respectively.

It is well-known that the pK_a value of PAA is about 4.[19] For pH < 4, many of the carboxyl groups are not dissociated and the PAA chains grafted onto the pore

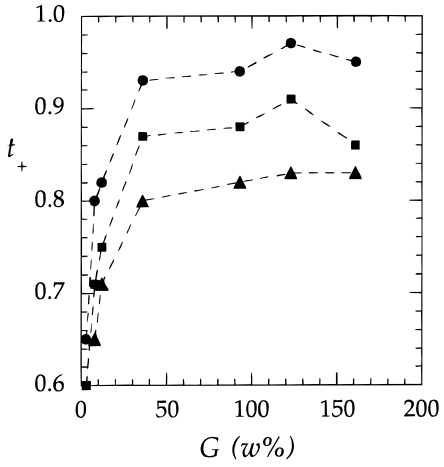

Figure 5. Potassium ion transport number as a function of grafting ratio for different KCl concentrations and no added HCl: 20 mM (●); 50 mM (■); 100 mM (▲).

surface collapse to increase their entropy.[20] The permeability is then very large and almost independent of the pH (see Figure 2). For pH > 4, most of the carboxyl groups are dissociated and the electrostatic repulsions between the negative charges bound to the PAA chains (presumably between charges along the same chain if the grafting ratio is not too high) are very important. The electrostatic energy can overcome now the entropic contribution to the free energy, which leads to an extension of the chain. This extension causes a blocking of the membrane pores and the concomitant reduction of the permeability (see Figures 1 and 2). When the PAA chains are in the extended form, the salt effect is very pronounced, since a high ionic strength solution screens the repulsive electrostatic interactions which causes the entropic contribution to prevail again. The permeability then increases with the salt concentration (see Figure 3). The final conformation of a polyacid chain lies now somewhere between the fully extended limit (corresponding to low salt concentration and high pH values) and the uncharged chain (corresponding to low pH values), so that the permeability for a given grafting ratio should remain lower than in the low pH case. In dilute solutions the less grafted membranes show the higher permeabilities, but this trend is not observed at high enough electrolyte concentrations because the hydrophobicity of the original, ungrafted PVDF membrane becomes more significant the more concentrated is the solution and the less grafted is the membrane.[17] This is clearly shown in Figure 3. Except for this effect, the grafting ratio generally influences the permeability in the trivial way; i.e., the permeability decreases when the grafting ratio increases.

From the above results it is clear that the charge density in the membrane should increase with the pH and salt concentration. However, for a fixed pH, the charge density increases less than the salt concentration does and this implies that the counterion transport number decreases with the salt concentration. This effect is shown in Figure 4. The influence of the grafting ratio on the counterion transport number is not so clear (see Figure 5). Increasing the grafting ratio should increase the charge density inside the membrane (and then the counterion transport number). However, ion-exchange capacity measurements[17] show clearly that only a fraction of the fixed acid groups can effectively contribute to the ion-exchange process. Although the grafting ratios studied are relatively low, the electrostatic interactions between charges[1,21,22] could be im-

portant, especially for those fixed groups adjacent to the hydrophobic PVDF surface. (Note that this surface is expected to have a very low electrical permittivity.) This saturation effect in the fixed charge density, together with a possible decrease of the ionic mobility with the grafting ratio, could explain why the counterion transport number first increases with the grafting ratio but reaches finally a nearly constant value at high enough (ca. 40%) grafting ratios.

Cooperative phenomena[23] between the units composing a polyacid chain can also be important here. At low charge density, the entropic contribution dominates and the chain adopts a random coil conformation. Increasing the charge density leads to an increase in the chain length due to electrostatic repulsion and the effect of the solvent (i.e., hydration of the chain increases when the acid groups are charged). Eventually, a minor increase in charge density will lead to a significant extension of the chain because electrostatic repulsion makes it difficult to accommodate additional charged groups in the random coiled form. Having a few charged units in the extended form can force a number of other units in the chain to change also to the extended form. The theory presented in the next section accounts for this cooperative phenomenon and explains the trends observed experimentally in membranes with low grafting ratios. However, important questions like the possibility of gel formation[17] and phase transitions[24] as well as the hysteresis properties of the chain length[19] have been left out of the theory. In particular, the minimum observed in the permeability with changing pH at higher grafting values (see Figure 2 here as well as Figure 5 of ref 17) cannot be properly explained at this preliminary stage. This minimum might be due to two opposite trends. On the one hand, an increase in the pH values causes a decrease in the membrane permeability due to the expansion of the PAA chains. On the other hand, the PAA chains can bind water molecules when ionized, which renders the membrane pore more hydrophilic. This latter effect acts to increase the permeability and is more noticeable for the higher grafting ratios, since in this case the PAA chains fill almost all of the pore. Note, finally, that the minimum is very marked for the higher grafting ratios (see Figure 5 of ref 17), which could suggest that interactions between the PAA chains grafted onto the pore surface become important in this case.[17]

III. Theory

III.1. Random Coiling and Stretching of a Single PAA Chain. We present here a simple model to explain the experimental trends observed. The model is based on the random coiling and stretching of a single PAA chain and does not include explicitly the effect of the grafting ratio. Accordingly, the first problem we examine is the evaluation of the chain length of a one-dimensional polyacid consisting of N units. Each unit carries a functional group and can be in one of the three following states: an uncharged state 0 corresponding to the (shortest) length l_0, a "short" charged state 1 of length $l_1 > l_0$, and a "long" charged state 2 of length $l_2 > l_1$. The first two states are preferred for entropic reasons: the short length in this one-dimensional model corresponds to a random coiled unit in the three-dimensional case, and random coiling arises because the configurational entropy of a polymer chain with a small end-to-end distance is much greater than that of the same chain with a large end-to-end distance.[20] The difference between l_0 and l_1 is assumed to be due to the higher hydration of the charged unit. It has been found that the degree of ionization is a principal factor in determining the hydration of PAA networks.[25] The long state 2 is the less favorable one from the point of view of entropy, but it could be preferred to the short state 1 when the electrostatic repulsion effects become dominant, since a larger distance between charges in the chain reduces its electrostatic energy. Note that it is the extension of the individual PAA chains rather than the swelling[17,26] of the PVDF matrix supporting the PAA chains which is assumed to be responsible for the behavior observed experimentally. Likewise, we consider that it is the pore-filling PAA chains, and not those chains grafted on the outer membrane surfaces, which dictate the membrane properties, at least for not too high grafting ratios. The PVDF matrix has a high porosity (ca. 75%), which facilitates diffusion of the acrylic acid and grafting of the membrane along the pore.[17]

In order to keep the model reasonably simple, we consider the partition function[27] $q(T)$ of a unit in state 0 to be equal to that of state 1 but greater than that of state 2, $q_2(T)$. Also, we take q_2 as the reference value ($q_2 = 1$). This accounts properly for the entropic contribution.[27] Next, we use a mean-field approximation[21,27] for the electrostatic interaction between nearest-neighbor charged units. And, finally, the number of configurations composed of charged units in states 1 and 2 is taken as the number of configurations possible for n_0 uncharged units out of the total number N of units composing the chain. The one-dimensional partition function Q of the chain takes then the form

$$Q = \frac{N!}{n_0!(N-n_0)!} q^{n_0+n_1} \times \exp\left\{-\frac{\omega_{11}{n_1}^2 + 2\omega_{12}n_1n_2 + \omega_{22}{n_2}^2}{NkT}\right\} \quad (1)$$

where n_i is the number of units in state i, ω_{ij} is the interaction energy between neighboring charged units in states i and j, k is the Boltzmann constant, and T is the absolute temperature. Note that $N = n_0 + n_1 + n_2$.

The interaction energies are modeled as in the Debye−Hückel theory, where the ratio of screened electrostatic energy to the thermal energy is given by[21,22,28]

$$\frac{\omega_{ij}}{kT} = \frac{e^2}{4\pi\epsilon_0\epsilon_r kT a_{ij}} \frac{e^{-a_{ij}/L_D}}{1 + a_{ij}/L_D} \quad (2)$$

where e is the electron charge, ϵ_0 is the vacuum permittivity, ϵ_r is the dielectric constant of the solvent ($\epsilon_r = 79$ in the case of water), a_{ij} is the effective distance for interaction between units in states i and j, and

$$L_D = \left(\frac{\epsilon_0\epsilon_r kT}{2e^2 N_A c}\right)^{1/2} \quad (3)$$

is the Debye length of the electrolyte solution. In eq 3, N_A is Avogadro's number and c is the molar concentration of the electrolyte in the solution. The distances a_{11} and a_{22} in eq 2 are equal to the lengths l_1 and l_2 defined previously, respectively, while $a_{12} \approx (a_{11} + a_{22})/2$.

The equilibrium conformational state of the one-dimensional polyacid chain will now be obtained for the following cases: (i) low pH, where the number of

charged units is so small that entropic effects prevail and no unit is in state 2; (ii) high pH and low concentrations, where the dominant electrostatic repulsion forces all the charged units to be in state 2; and, finally, (iii) the general case where the three states are populated.

Case i, $n_2 = 0$. The chain partition function simplifies now to

$$Q = \frac{N!}{n_0!(N-n_0)!} q^N \exp\left\{-\frac{\omega_{11}(N-n_0)^2}{NkT}\right\} \quad (4)$$

and the equilibrium number of uncharged units n_0 is determined by equating the chemical potential of the hydrogen ions in the −COOH groups of the chain

$$\mu_{H^+}(-COOH) = -kT\frac{\partial \ln Q}{\partial n_0} \approx kT\left(\ln \frac{n_0}{N-n_0} - 2\frac{\omega_{11}(N-n_0)}{NkT}\right) \quad (5)$$

to the chemical potential of these ions in the membrane solution

$$\mu_{H^+}(H_3O^+) = \mu^0_{H^+} + kT \ln [H_3O^+] + e\phi_D \quad (6)$$

where $\mu^0_{H^+}$ is the standard chemical potential of hydrogen ions in the membrane solution, $[H_3O^+]$ is the concentration of the ions in this solution, and ϕ_D is the Donnan potential.[29,30] Note that $\phi_D = \phi$(solution) − ϕ(membrane) is positive because the membrane is negatively charged and the electric potential ϕ has been set equal to zero in the membrane phase. Stirling's approximation[27] has been used in eq 5. From eqs 5 and 6, n_0 is given by the implicit equation

$$\frac{[H_3O^+]e^{e\phi_D/kT}}{K_a} = \frac{n_0}{N-n_0}\exp\left\{-\frac{2\omega_{11}(N-n_0)}{NkT}\right\} \quad (7)$$

where $K_a \equiv \exp(-\mu^0_{H^+}/kT)$. Equation 7 constitutes a mass action law corrected for the interaction between charged units ($\omega_{11} \neq 0$), as well as for the difference in pH between the bathing solution and the membrane solution ($\phi_D \neq 0$). However, this latter correction (i.e., the factor $e^{e\phi_D/kT}$ on the left hand side of eq 7) is small here. Indeed, bearing in mind that most of the results in Figure 5 correspond to a membrane fixed charge concentration close to the external solution concentration, i.e., of the order of 0.1 M, it can easily be proved[28] that the pH in the membrane phase is smaller than the pH in the bathing solution by $e\phi_D/(2.303kT) \approx 0.2$ units, an effect that can be neglected except for the case of very dilute external solutions where ϕ_D can take higher values.

In eq 7, the acidity constant K_a of the polyacid is defined as $\exp(-\mu^0_{H^+}/kT)$ because this standard chemical potential has been defined with reference to the state of the hydrogen in the chain. Thus, n_0 increases with decreasing pH and increasing electrostatic repulsion energy ω_{11}. Note that there are no entropic effects in this case because states 0 and 1 are equally preferred from the point of view of entropy.

Case ii, $n_1 = 0$. The chain partition function reduces now to

$$Q = \frac{N!}{n_0!(N-n_0)!} q^{n_0} \exp\left\{-\frac{\omega_{22}(N-n_0)^2}{NkT}\right\} \quad (8)$$

and the equilibrium number of uncharged units is given by

$$\frac{[H_3O^+]}{K_a} = \frac{n_0}{N-n_0}\frac{1}{q}\exp\left\{-\frac{2\omega_{22}(N-n_0)}{NkT}\right\} \quad (9)$$

which is again a mass action law corrected now for the interaction between charged units as well as for the entropic preference for the uncharged states ($q > 1$).

Case iii, $n_1 \neq 0$ and $n_2 \neq 0$. The equilibrium number of charged units in short and long states is now obtained by equating the chemical potential of the units in these two states

$$\mu_1 = -kT\frac{\partial \ln Q}{\partial n_1} = -kT\frac{\partial \ln Q}{\partial n_2} = \mu_2 \quad (10)$$

which, after use of eq 1, gives

$$(\omega_{11} - \omega_{12})n_1 + (\omega_{12} - \omega_{22})n_2 = \frac{NkT}{2}\ln q \quad (11)$$

Since $a_{11} < a_{12} < a_{22}$ and $\omega_{11} > \omega_{12} > \omega_{22}$ (see eq 2), the coefficients of n_1 and n_2 in eq 11 are positive.

The chemical potential of the hydrogen ions in the −COOH groups is now calculated as

$$\mu_{H^+}(-COOH) = -kT\frac{\partial \ln Q}{\partial n_0} \approx kT\left(\ln \frac{n_0}{N-n_0} - \frac{\omega_{11}-\omega_{12}}{\Delta\omega}\ln q - \frac{2(N-n_0)(\omega_{11}\omega_{22} - \omega_{12}^2)}{NkT\Delta\omega}\right) \quad (12)$$

where $\Delta\omega \equiv \omega_{11} + \omega_{22} - 2\omega_{12}$ and the partial derivative is constrained by the restriction of eq 11 and the condition $N = n_0 + n_1 + n_2$. The equilibrium number of uncharged units is then given by

$$\frac{[H_3O^+]}{K_a} = \frac{n_0}{N-n_0} q^{-(\omega_{11}-\omega_{12})/\Delta\omega} \times \exp\left\{-\frac{2(N-n_0)(\omega_{11}\omega_{22} - \omega_{12}^2)}{NkT\Delta\omega}\right\} \quad (13)$$

which reduces to eqs 7 and 9 in the limiting cases $\omega_{11} = \omega_{12}$ and $\omega_{12} = \omega_{22}$, respectively.

The method used to solve the above equations is as follows. First, we assume that equilibrium between the two charged states has been attained (i.e., that eq 11 is satisfied). We then solve eq 13 for the fraction of uncharged units n_0/N and introduce the result in the condition $N = n_0 + n_1 + n_2$, which can finally be used together with eq 11 to evaluate the fractions of charged units n_1/N and n_2/N. If any of these two fractions is negative, this means that the initial assumption of equilibrium between the charged states was wrong and only one of these two states was occupied. In this case, we evaluate again n_0/N, using now either eq 7 (if n_2/N was negative) or eq 9 (if n_1/N was negative). The length of the PAA chain is finally given by

$$l_{PAA} = N\left(\frac{n_0}{N}l_0 + \frac{n_1}{N}l_1 + \frac{n_2}{N}l_2\right) \quad (14)$$

where N remains to be evaluated from the grafting ratio. Note that, according to previous experimental results, the model assumes that the principal factor dictating the configuration of the grafted chains is the electrostatic force among the dissociated carboxyl groups.[17,26,30]

III.2. Permeability of the PVDF/PAA Membrane. We model the membrane as a parallel assembly of cylindrical capillaries of radius r.[18] According to the Hagen−Poiseuille law, the volume flow through the membrane when a pressure difference Δp is applied externally is given by[12,31]

$$\dot{V} = N_p \frac{\pi r^4 \Delta p}{8\eta d} \tag{15}$$

where d is the membrane thickness (i.e., the length of the capillaries), η is the solvent viscosity ($\eta = 1.0$ mPa·s in the case of water), and N_p is the number of pores in the membrane. We define the membrane permeability as

$$P \equiv \frac{\dot{V} d}{A_g \Delta p} = \frac{\epsilon r^2}{8\eta} \tag{16}$$

where A_g is the exposed geometrical area of the membrane and $\epsilon \equiv N_p \pi r^2 / A_g$ is the porosity of the membrane. Porosity and water permeability measurements of ungrafted PVDF membranes allow the evaluation of the density of pores N_p/A_g and the effective capillary radius for water permeability, r_{PVDF}. We assume that the grafting of the membrane leads to a decrease of this capillary radius from $r = r_{PVDF}$ to $r = r_{PVDF} - l_{PAA}$, where l_{PAA} is given by eq 14, and therefore to a decrease in the permeability according to eq 16. This assumption is motivated by previous SEM micrographs,[17] which showed that while the pore size is reduced when the grafting ratio increases, the grafted PAA chains do not totally block the pores.

III.3. Predictions of the Model. Let us analyze first the trends predicted by the model and the influence of the different parameters. This will be done by evaluating most of the parameters from the present experimental results and giving approximate values to the other parameters in the theory.

The original porosity of the PVDF membrane[17,32] is about 75% (i.e., $\epsilon = 0.75$) and its water permeability is $P = 7.0 \times 10^{-7}$ cm^2 Pa^{-1} s^{-1}, as calculated from the manufacturer's data.[32] Equation 16 gives then the effective capillary radius for water permeability as $r_{PVDF} = 0.86\ \mu$m and the effective density of pores as $N_p/A_g = 3.2 \times 10^7$ cm^{-2}. The effective capillary radius is about one-third of the nominal pore radius, which should be ascribed to the capillary membrane model used here:[6,18] the tortuous path of the water molecules through the hydrophobic membrane is simulated in this model by an effective radius smaller than the nominal one.

According to eq 16, the permeability of the PVDF/PAA membranes will then be given by

$$P = 1.3 \times 10^{-6}(0.86 - l_{PAA})^4 \text{ cm}^2 \text{ Pa}^{-1} \text{ s}^{-1} \tag{17}$$

where l_{PAA} (μm) is calculated from eq 14. Figure 6 shows a plot of P against pH for an ionic strength of 100 mM (the same as in Figure 2) and different values of the entropy parameter q. The other parameters in the theory have tentatively been taken as p$K_a = 3.5$, $l_0 = 3$ Å, $l_1 = a_{11} = 3.5$ Å, $l_2 = a_{22} = 6$ Å, $a_{12} = 4.75$ Å, and $N = 1300$. The pK_a value of PAA is about 4.[19] Model networks[26] of PAA indicate, however, that the degree of ionization reaches its half-maximum value in the vicinity of pH 5. Another study[33] has reported that the most pH-sensitive change of water permeability was observed at pH ca. 3 with PAA-grafted porous membranes. The difference between the solution and the membrane pK_a values is probably due to the locally high charge density inside the grafted pore.[34] The values for l_0, l_1, and l_2 were estimated by using a simple molecular modeling software package (Alchemy III): it must be realized that these are not exact values but represent only reasonable approximations. The value for N should be regarded as the "effective" number of units in a chain. Figure 7 shows a plot of P against c for different values of parameter q. The pH has been set to 5.8 (as in Figure 3), and the other parameters are those used for Figure 6. When comparing Figures 6 and 7 to Figures 2 and 3, we see that the model is capable of reproducing the experimental trends observed for a particular choice of the adjustable parameters. In particular, we have rationalized theoretically the experimental fact that the membrane permeability can increase by several orders of magnitude by changing the external pH and salt concentration. We cannot, however, give an explanation for the minimum observed in Figure 2 and Figure 5 of ref 17 since this effect is partly due to interactions between different PAA chains, and we have only considered the conformation of a single PAA chain here. The model is not thus suitable for membranes having high grafting ratios.

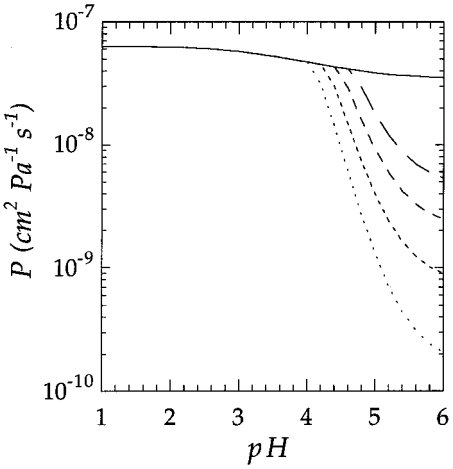

Figure 6. Membrane permeability at constant ionic strength of 100 mM as a function of pH for the values of the entropy parameter $q = 1.6$ (···), 1.7 (---), 1.8 (− − −), 1.9 (— — —), and ∞ (—).

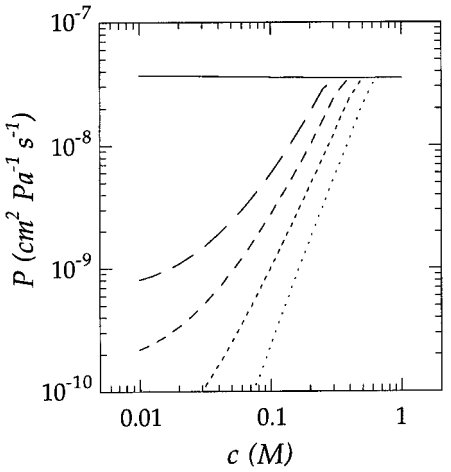

Figure 7. Membrane permeability as a function of salt concentration for pH = 5.8 and the values of the entropy parameter $q = 1.6$ (···), 1.7 (---), 1.8 (− − −), 1.9 (— — —) and ∞ (—).

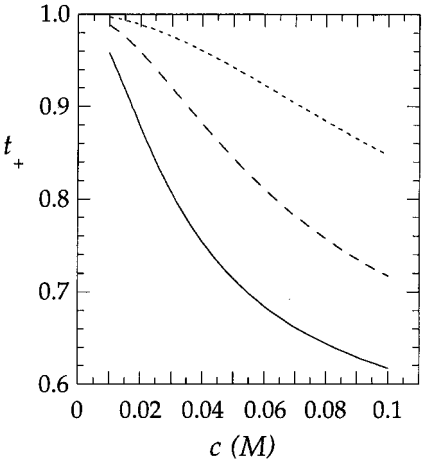

Figure 8. Potassium transport number as a function of KCl concentration for pH = 5.8 and the values of X_M = 50 mM (—), 100 mM (---) and 200 mM (···).

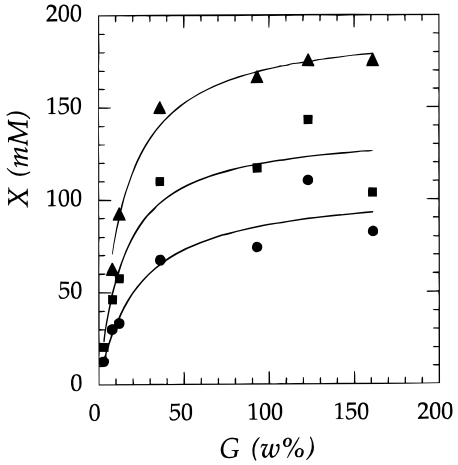

Figure 9. Membrane fixed charge concentration as a function of percent grafting for different KCl concentrations and no added HCl: 20 mM (●); 50 mM (■); 100 mM (▲).

The entropy parameter q is related to the random coiling of the PAA chain: an increase in q corresponds to a more coiled chain conformation and, therefore, to an increase in the membrane permeability at given pH and concentration values. As could be anticipated, the sensitivity of the permeability to pH and concentration changes decreases with q.

The anomalous dependence of the permeability on the grafting ratio observed for concentrated solutions (see Figure 3) and also the minimum of Figure 2 might be quantitatively described by eqs 15−17 if we were to introduce a membrane partition coefficient[18] accounting for the hydrophilicity of the ionized PAA chains. This effect should be more pronounced the higher the grafting ratio is, and thus the permeabilities of Figure 3 reach similar values in the high-concentration range despite the very different grafting ratios of the membranes. In this range, many of the PAA chains adopt the random coiled form, and thus it is the hydrophilic nature of the ionized chains rather than the chain length which dictates the permeability. However, since the model should not be applied to high grafting ratios, we will not attempt any modeling of this effect here. In addition, it is likely that the PAA chains grafted on the outer membrane surfaces (and not only those grafted on the pore surface) influence the transport through the membrane at high grafting ratios, and these layers have been omitted in our model.

Figure 8 shows the potassium transport number vs KCl concentration c in the bathing solution (see Figure 4 for comparison). The transport numbers in Figure 8 have been evaluated by assuming $D_+ \approx D_-$, where the subscripts refer to the potassium (+) and chloride (−) ions, and using the Donnan equilibrium theory[31] for the ion concentrations c_+ and c_- in the membrane, which leads to

$$t_+ = \frac{D_+c_+}{D_+c_+ + D_-c_-} \approx \frac{c_+}{c_+ + c_-} = \frac{1}{2}\left\{1 + \frac{1}{[1 + (2c/X)^2]^{1/2}}\right\} \quad (18)$$

In eq 18, X is the membrane-fixed charge concentration, which has been estimated here as

$$X = X_M\left(\frac{n_1}{N} + \frac{n_2}{N}\right) \quad (19)$$

where X_M represents the maximum fixed charge concentration and n_1 and n_2 are evaluated from the equations in the preceding section. It has been found that $n_1 + n_2$ is not very sensitive to q, and therefore only the curves corresponding to $q \rightarrow \infty$ are shown in Figure 8. Also, the parameter X_M has been given the tentative values 50, 100, and 200 mM. In principle, X_M should increase with the grafting ratio[17] though the actual dependence is unknown.

Figure 9 gives the empirical function X vs G which results from the fitting of t_+ (eq 18) to the results in Figure 5. As anticipated previously (see Figure 5), the saturation effect observed in Figure 9 could indicate that only the fraction of the fixed charge groups far from the hydrophobic, low electrical permittivity PVDF surface are responsible for the ion-exchange characteristics of the membrane. We see from Figure 9 that when $G \geq$ 30% the membrane is grafted throughout, and a further increase of the G values causes no increase in X. A previous study[34] has also found a leveling-off tendency of the X vs G curve at high grafting ratios, though no saturation effect was observed there. This tendency was explained in terms of the grafts located on the outer membrane surfaces:[34] for the fraction of grafts located on these surfaces an increase in the number of ion-exchange groups could be offset by an increase in volume due to swelling. We see again that our omission of a PAA layer on the outer membrane surface might not be justified for high values of G.

IV. Conclusions

A very simple theoretical model describing the effects of pH and salt concentration on the permeability and counterion transport number of a VPM has been presented and tested experimentally for the case of graft-modified PVDF/PAA membranes with low grafting ratios. The theory assumes the random coiling and stretching of a single PAA chain to be the main mechanism responsible for the membrane behavior: studying the statistical conformations of a polyacid chain grafted onto the membrane pore surface leads to an explanation for most of the observed experimental trends on a semiquantitative basis. In particular, the fact that the membrane permeability changes by several orders of magnitude when the pH and salt concentration of the external solution are varied can be rationalized in terms of very simple physical principles. For the case of membranes with high grafting ratios, however, it

seems that not only the conformation of a single chain but also the interaction among chains[17] as well as the possibility of having PAA layers on the outer membrane surfaces[34] must be considered in order to explain the experimental data. In this context, future work should address the question of the location of the graft polyelectrolyte in the porous membrane when high grafting ratios[17,34] are employed.

Acknowledgment. Financial support from DGICYT, Ministry of Education and Science of Spain, under project No. PB95-0018 for J.A.M. and S.M. and from TEKES (The Technological Development Center in Finland) for K.K. and P.V. is gratefully acknowledged.

References and Notes

(1) Grodzinsky, A. J. *CRC Crit. Rev. Biomed. Eng.* **1983**, *9*, 133.
(2) Osada, Y. *Adv. Polym. Sci.* **1987**, *82*, 1.
(3) Otero, T. F.; Rodríguez, J.; Angulo, E.; Santamaría, C. *Synth. Met.* **1993**, *55−57*, 3713. Otero, T. F.; Rodríguez, J. *Intrinsically Conducting Polymers: An Emerging Technology*; Aldissi, M., Ed.; Kluwer Academic Publishers: Dordrecht, The Netherlands, 1993; p 179.
(4) Gong, J. P.; Nitta, T.; Osada, Y. *J. Phys. Chem.* **1994**, *98*, 9583.
(5) Maršik, F.; Mejsnar, J. *J. Non-Equilib. Thermodyn.* **1994**, *19*, 197.
(6) Nishi, S.; Kotaka, T. *Macromolecules* **1986**, *19*, 978.
(7) Grimshaw, P. E.; Nussbaum, J. H.; Grodzinsky, A. J.; Yarmush, M. L. *J. Chem. Phys.* **1990**, *93*, 4462.
(8) Casolaro, M.; Barbucci, R. *Colloids Surf. A* **1993**, *77*, 81.
(9) Shoenfeld, N. A.; Grodzinsky, A. J. *Biopolymers* **1980**, *19*, 241.
(10) Eisenberg, S. R.; Grodzinsky, A. J. *J. Membr. Sci.* **1984**, *19*, 173.
(11) Brøndsted, H.; Kopeček, J. In *Polyelectrolyte Gels*; Harland, R. S., Prud'homme, R. K., Eds.; ACS Symposium Series 480; American Chemical Society: Washington, DC, 1992; Chapter 17.
(12) Kim, J. T.; Anderson, J. L. *J. Membr. Sci.* **1989**, *47*, 163.
(13) Ly, Y.; Cheng, Y.-L. *J. Membr. Sci.* **1993**, *77*, 99.
(14) Morris, D. R.; Sun, X.; Yang, L. In *Polyelectrolyte Gels*; Harland, R. S., Prud'homme, R. K., Eds.; ACS Symposium Series 480; American Chemical Society: Washington, DC, 1992; Chapter 14.
(15) Leung, S.-H.; Robinson, J. R. In *Polyelectrolyte Gels*; Harland, R. S., Prud'homme, R. K., Eds.; ACS Symposium Series 480; American Chemical Society: Washington, DC, 1992; Chapter 16.
(16) Grimshaw, P.E.; Grodzinsky, A. J.; Yarmush, M. L.; Yarmush, D. M. *Chem. Eng. Sci.* **1990**, *45*, 2917.
(17) Hautojärvi, J.; Kontturi, K.; Näsman, J. H.; Svarfvar, B. L.; Viinikka, P.; Vuoristo, M. *Ind. Eng. Chem. Res.* **1996**, *35*, 450.
(18) Verbrugge, M. W.; Pintauro, P. N. In *Modern Aspects of Electrochemistry*; Conway, B. E., Bockris, J. O., White, R. E., Eds.; Plenum: New York, 1989; Vol. 19, p 1.
(19) Harada, J.; Chern, R. T.; Stannet, V. T. *Polyelectrolyte Gels*; Harland, R. S., Prud'homme, R. K., Eds.; ACS Symposium Series 480; American Chemical Society: Washington, DC, 1992; Chapter 5.
(20) de Gennes, P. G. *Scaling Concepts in Polymer Physics*; Cornell University Press: Ithaca, NY, 1979; Chapter 1. Yamakawa, H. *Modern Theory of Polymer Solutions*; Harper & Row: New York, 1971; Chapter 2.
(21) Mafé, S.; Manzanares, J. A.; Reiss, H. *J. Chem. Phys.* **1993**, *98*, 2325.
(22) Nishio, T. *Biophys. Chem.* **1991**, *40*, 19.
(23) Engel, J. In *Biophysics*; Hoppe, W., Lohmann, W., Markl, H., Ziegler, H., Eds.; Springer-Verlag: Berlin, 1983; pp 233−43.
(24) Tanaka, T. In *Polyelectrolyte Gels*; Harland, R. S., Prud'homme, R. K., Eds.; ACS Symposium Series 480; American Chemical Society: Washington, DC, 1992; Chapter 1. Tanaka, T.; Fillmore, D.; Sun, S.-T.; Nishio, I.; Swislow, G.; Shah, A. *Phys. Rev. Lett.* **1980**, *45*, 1636. Ohmine, I.; Tanaka, T. *J. Chem. Phys.* **1982**, *77*, 5725.
(25) Oppermann, W. In *Polyelectrolyte Gels*; Harland, R. S., Prud'homme, R. K., Eds.; ACS Symposium Series 480; American Chemical Society: Washington, DC, 1992; Chapter 10.
(26) Shefer, A.; Grodzinsky, A. J.; Prime, K. L.; Busnel, J. P. *Macromolecules* **1993**, *26*, 5009.
(27) Hill, T. L. *An Introduction to Statistical Thermodynamics*; Dover: New York, 1986; Chapter 14.
(28) Minakata, A.; Matsamura, K.; Sasaki, S.; Ohmuna, H. *Macromolecules* **1980**, *13*, 1549. Cleland, R. L. *Macromolecules* **1984**, *17*, 634. Zhang, L.; Takematsu, T.; Norisuye, T. *Macromolecules* **1987**, *20*, 2882.
(29) Reiss, H. *J. Phys. Chem.* **1988**, *92*, 3657. Chartier, P.; Mattes, B.; Reiss, H. *J. Phys. Chem.* **1992**, *96*, 3556. Mafé, S.; Manzanares, J. A.; Reiss, H. *J. Chem. Phys.* **1993**, *98*, 2408.
(30) Islam, M. A.; Dimov, A.; Malinova, A. L. *J. Membr. Sci.* **1992**, *66*, 69.
(31) Laksminarayanaiah, N. *Equations of Membrane Biophysics*; Academic Press: New York, 1984; Chapter 3.
(32) *The Millipore Catalogue*; Millipore Co.: Bedford, MA, 1987; p 23.
(33) Ito, Y.; Inaba, M.; Chung, D. J.; Imanishi, Y. *Macromolecules* **1992**, *25*, 7313.
(34) Mika, M.; Childs, R. F.; Dickson, J. M.; McCarry, B. E.; Gagnon, D. R. *J. Membr. Sci.* **1995**, *108*, 37.

MA960501Y